Noise-driven interfaces and their macroscopic representation

Marco Dentz, Insa Neuweiler, Yves Méheust, and Daniel M. Tartakovsky

Phys. Rev. E **94**, 052802 — Published 7 November 2016

DOI: 10.1103/PhysRevE.94.052802

Noise-Driven Interfaces and Their Macroscopic Representation

Marco Dentz
*Spanish National Research Council (IDAEA-CSIC), 08034 Barcelona, Spain**

Insa Neuweiler
Institute of Fluid Mechanics in Civil Engineering, Leibniz University Hanover, Hanover, Germany

Yves Méheust
Geosciences Rennes, UMR 6118, Université de Rennes 1, CNRS, Rennes, France

Daniel M. Tartakovsky
Department of Mechanical and Aerospace Engineering, University of California, San Diego, 9500 Gilman Drive, La Jolla, CA 92093, USA†

We study the macroscopic representation of noise-driven interfaces in stochastic interface growth models in $(1+1)$ dimensions. The interface is characterized macroscopically by saturation, which represents the fluctuating sharp interface by a smoothly varying phase field with values between 0 and 1. We determine the one-point interface height statistics for the Edwards-Wilkinson (EW) and Kadar-Paris-Zhang (KPZ) models in order to determine explicit deterministic equations for the phase saturation for each of them. While we obtain exact results for the EW model, we develop a Gaussian closure approximation for the KPZ model. We identify an interface compression term, which is related to mass transfer perpendicular to the growth direction, and a diffusion term that tends to increase the interface width. The interface compression rate depends on the mesoscopic mass transfer process along the interface and in this sense provides a relation between meso and macroscopic interface dynamics. These results shed new light on the relation between mesoscale and macroscale interface models, and provide a systematic framework for the upscaling of stochastic interface dynamics.

PACS numbers: 05.40.–a

I. INTRODUCTION

Dynamics of fluctuating interfaces is central to understanding and quantification of growth phenomena in a plethora of disciplines ranging from material science to biology, and plasma physics to hydrology. Studies of interface growth and dynamics deal with phenomena as diverse as immiscible fluid displacement [1, 2], biofilm growth and evolution of bacterial colonies [3], crystal growth [4] and sediment deposition, as well as the morphogenesis of interosseous structures [5]. While the underlying (physical, chemical, or biological) mechanisms of these and other interfacial phenomena can be quite different, the focus on fluctuating interface dynamics facilitates the development of general approaches.

Fluctuations of the interface height are described by stochastic differential equations, such as the random deposition model [6], the Edwards-Wilkinson (EW) model, and the Kadar-Parisi-Zhang (KPZ) model. These approaches have been used to describe such interfacial growth phenomena as molecular beam epitaxy, biofilm growth, and combustion fronts [7], fluctuating fluid interfaces [8], movement of fluid interfaces in disordered media [2, 6, 9], and reaction fronts in disordered flows [10]. Reviews of such stochastic models can be found in [1, 6, 9, 11].

These models describe the interface behavior under different growth mechanisms, and quantify the impact of system fluctuations driven by spatial and temporal disorder on the growth and displacement dynamics. Phase saturation, or occupancy maps [12–14], on the other hand, provide macroscopic descriptions of the interface evolution. For $(1+1)$–dimensional interfaces, phase saturation $S(z,t)$ at the longitudinal position z and time t is defined in terms of the interface height, $z = H(x,t)$, as

$$S(z,t) = \frac{1}{2a}\int_{-a}^{a} \mathcal{H}[H(x,t)-z]\mathrm{d}x \qquad (1)$$

where $\mathcal{H}(\cdot)$ is the Heaviside function, x is the transverse coordinate, and $2a$ is the domain size. The mesoscale description, $H(x,t)$, exhibits significant fluctuations, while its macroscopic (phase-field) representation, $S(z,t)$, varies smoothly between 0 and 1. We address the hitherto open question of how to account for mesoscale interface fluctuations with lateral relaxation in macroscopic saturation models. Thus, the objective of this paper is to investigate the macroscopic (deterministic) saturation dynamics which originate in mesoscale (stochastic) interface fluctuations.

*Electronic address: marco.dentz@csic.es
†Electronic address: dmt@ucsd.edu

We consider the $(1+1)$–dimensional KPZ model [15]

$$\frac{\partial H}{\partial t} = v + \kappa \frac{\partial^2 H}{\partial x^2} + \frac{\lambda}{2}\left(\frac{\partial H}{\partial x}\right)^2 + \xi(x,t), \qquad (2)$$

which describes the evolution of the interface height $H(x,t)$ due to the combined effects of a constant growth rate v, the interface relaxation process (transverse redistribution of mass) represented by the second (EW) term, the transverse interface growth encoded in the third (KPZ) term, and the Gaussian white noise $\xi(x,t)$. The latter has zero mean, variance σ_ξ^2, and a two-point correlation $\langle \xi(x,t)\xi(x',t')\rangle = 2Dl_0\delta(x-x')\delta(t-t')$ where l_0 is a characteristic fluctuation scale, and $\delta(\cdot)$ is the Dirac delta function. The EW model [16] corresponds to (2) with $\lambda = 0$.

II. PHASE SATURATION AND INTERFACE STATISTICS

When the transverse system size $2a$ significantly exceeds the characteristic fluctuation length l_0, $a \gg l_0$, the spatial average in (1) is equivalent to the ensemble average $\langle\cdot\rangle$. In other words, the phase saturation S at a position z corresponds to the probability that $H(x,t) > z$,

$$S(z,t) = \int_z^\infty p_H(h,t)\mathrm{d}h, \qquad (3)$$

where $p_H(h,t)$ is the probability density function (PDF) of the interface height at time t.

A. Multi-point Probability Density Function

Our derivation of an equation for the PDF of $H(x,t)$ starts with a spatial discretization of (2). Since the treatment of $\xi(x,\cdot)$ as a white noise may be considered an idealization corresponding to $l_0 \ll a$, we choose l_0 as the discretization scale. Then the interface height $H(x,t)$ is represented by a vector $\mathbf{H}(t) = [\ldots, H_{-i}(t), \ldots, H_i(t), \ldots]^\top$, and (2) gives rise to the multi-dimensional Langevin equation [17]

$$\frac{\mathrm{d}H_i}{\mathrm{d}t} = v + E_i(\mathbf{H}) + K_i(\mathbf{H}) + \xi_i(t). \qquad (4)$$

Here we have defined

$$H_i \equiv \frac{1}{l_0}\int_{x_i}^{x_i+l_0} H(x,t)\mathrm{d}x, \quad \xi_i \equiv \frac{1}{l_0}\int_{x_i}^{x_i+l_0} \xi(x,t)\mathrm{d}x. \qquad (5)$$

and $E_i(\mathbf{H})$ and $K_i(\mathbf{H})$ are, respectively, discretized versions of the EW and KPZ terms

$$E_i(\mathbf{H}) = \kappa\frac{H_{i+1} + H_{i-1} - 2H_i}{l_0^2} \qquad (6)$$

$$K_i(\mathbf{H}) = \frac{\lambda}{2}\frac{(H_{i+1} - H_{i-1})^2}{4l_0^2}. \qquad (7)$$

Note that the noise covariance is given by

$$\langle \xi_i(t)\,\xi_j(t')\rangle = 2D\delta_{ij}\delta(t-t'), \qquad (8)$$

where δ_{ij} is the Kronecker delta function. The discretization scheme (7) provides stable numerical solutions for moderate non-linearity [17–19]. For strong coupling alternative numerical discretization schemes need to be employed [18, 20].

In the limit $a \gg \ell_0$, the interface height statistics are stationary. This means, the mean height $\langle H_i\rangle = \langle H\rangle$ is independent from the position, and the height covariance, which is defined by

$$C_{ij} = \langle (H_i - \langle H_i\rangle)\,(H_j - \langle H_j\rangle)\rangle \qquad (9)$$

is a function of $|i-j|$ only. The interface height variance C_{ii} is denoted by

$$\sigma_H^2 \equiv C_{ii}. \qquad (10)$$

The evolution of the joint PDF of $\mathbf{H}(t)$, $p_{\mathbf{H}}(\mathbf{h},t)$, is governed by the Fokker-Planck equation equivalent to (4),

$$\frac{\partial p_{\mathbf{H}}}{\partial t} = D\nabla_{\mathbf{h}}^2 p_{\mathbf{H}} - \sum_i \frac{\partial U_i p_{\mathbf{H}}}{\partial h_i}, \qquad (11)$$

where we defined the drift

$$U_i(\mathbf{h}) = v + E_i(\mathbf{h}) + K_i(\mathbf{h}). \qquad (12)$$

A similar perspective on the interfacial growth phenomenon can be found in [21], which derives Langevin equations for fluctuating surfaces from master equations that describe the evolution of the joint PDF of the interface heights.

B. One-Point Probability Density Function

The phase saturation, as defined by (3), requires the determination of the single-point PDF, $p_{H_i}(h_i,t)$, of the interface height $H_i(t) \equiv H(x_i,t)$. It is obtained by marginalization of $p_{\mathbf{H}}(\mathbf{h},t)$, i.e.,

$$p_{H_i}(h_i,t) = \prod_{j\neq i}\int p_{\mathbf{H}}(\mathbf{h},t)\mathrm{d}h_j. \qquad (13)$$

Integration of (11) over all h_j with $j \neq i$ gives

$$\frac{\partial p_{H_i}}{\partial t} = D\frac{\partial^2 p_{H_i}}{\partial h_i^2} - \frac{\partial V_i p_{H_i}}{\partial h_i}, \qquad (14)$$

where we defined the conditional drift

$$V_i = v + \langle E_i(\mathbf{H})|h_i\rangle + \langle K_i(\mathbf{H})|h_i\rangle. \qquad (15)$$

The conditional averages are of the form

$$\langle f(H_j)|H_i = h_i\rangle = \int f(h_j)p_{H_j|H_i}(h_j,t|h_i)\mathrm{d}h_j, \qquad (16)$$

where $f[H_j(t)]$ is any function of the interface height $H_j(t)$ at point $j \neq i$. Since the conditional PDF

$$p_{H_j|H_i}(h_j, t|h_i) = \frac{p_{H_i,H_j}(h_i, h_j, t)}{p_{H_i}(h_i, t)} \tag{17}$$

is in principle unknown, the drift velocity U is not computable and (14) requires a closure. Note that for the sake of clarity we maintained here the index i for the PDF of H_i. Due to stationarity, however, the one-point PDF is independent of position.

III. CLOSURES

We first consider the exactly solvable random deposition and EW models before addressing the KPZ model by means of a closure approximation.

A. Random Deposition Model

For the random deposition model, $\lambda = \kappa = 0$. Thus, the solution for the equation for the single point height PDF $p_H(h, t)$ is given by the advection-dispersion equation

$$\frac{\partial p_H}{\partial t} = D\frac{\partial^2 p_H}{\partial h^2} - v\frac{\partial p_H}{\partial h}. \tag{18}$$

The equation for the phase saturation $S(z, t)$ defined by (3) is thus given by

$$\frac{\partial S}{\partial t} = D\frac{\partial^2 S}{\partial z^2} - v\frac{\partial S}{\partial z}, \tag{19}$$

Its solution for the initial condition $S(z, t = 0) = \Theta(z)$ with $\Theta(z)$ the Heaviside step function is given by

$$S = \frac{1}{2}\mathrm{erfc}\left(\frac{z - vt}{\sqrt{4Dt}}\right). \tag{20}$$

B. Edwards-Wilkinson Model

For the EW model, i.e., for $\lambda \equiv 0$ in (2), the discretized evolution equation (4) is a multi-dimensional Ornstein-Uhlenbeck process [22]. In this case, and for the known (deterministic) initial height distribution $p_{\mathbf{H}}(\mathbf{h}, t = 0) = \delta(\mathbf{h})$, the joint PDF $p_{\mathbf{H}}(\mathbf{h}, t)$ is a multivariate Gaussian. In this case, the conditional PDF $p_{H_j|H_i}(h_j, t|h_i)$ is known and given by a Gaussian PDF whose mean is

$$\langle H_j|h_i\rangle = \langle H\rangle + \frac{C_{ij}}{C_{ii}}\left(h_i - \langle H\rangle\right). \tag{21}$$

The unconditional height covariances C_{ij} are defined by (9). Thus, we can close equation (14) for the one point interface height through the exact calculation of the conditional moments in the drift (15) for $\kappa \equiv 0$. This gives

$$V_i(h_i) = v + \frac{\mathcal{E}_i}{\sigma_H^2}\left(h_i - \langle H\rangle\right), \tag{22}$$

where we defined

$$\mathcal{E}_i = \kappa\frac{C_{ii+1} - 2C_{ii} + C_{ii-1}}{\ell_0^2}. \tag{23}$$

This expression is obtained by using (21) to determine the conditional averages in $\langle E_i(\mathbf{H})|h_i\rangle$ with $E_i(\mathbf{H})$ given by (6). We can relate $\mathcal{E}_i$ to the variance $C_{ii} = \sigma_H^2$ by using (4) for $\lambda = 0$. First, we note that the mean height is given by $\langle H\rangle = vt$. Thus, we obtain from (4) for the head fluctuation $H' = H - \langle H\rangle$

$$\frac{\mathrm{d}H_i'}{\mathrm{d}t} = E_i(\mathbf{H}') + \sqrt{2D}\xi_i(t). \tag{24}$$

Multiplication of the latter with H_i' and using the Ito rule gives

$$\frac{\mathrm{d}\sigma_H^2}{\mathrm{d}t} = \mathcal{E}_i + 2D. \tag{25}$$

Thus, we obtain for the drift $V_i(h_i)$ the closed form expression

$$V_i = v + \left[\frac{\mathrm{d}\ln(\sigma_H^2)}{\mathrm{d}t} - \frac{2D}{\sigma_H^2}\right](h_i - vt), \tag{26}$$

In the following, we define for compactness

$$\gamma \equiv \frac{2D}{\sigma_H^2} - \frac{\mathrm{d}\ln(\sigma_H^2)}{\mathrm{d}t}. \tag{27}$$

The evolution of the variance σ_H^2 of the interface height has been well-known [23] and is given by

$$\sigma_H^2 = \frac{2D\ell_0\sqrt{t}}{\sqrt{2\pi\kappa}}. \tag{28}$$

We thus obtain for the one-point PDF $p_H(h, t)$ the evolution equation

$$\frac{\partial p_H}{\partial t} = D\frac{\partial^2 p_H}{\partial h^2} - \frac{\partial\left[v - \gamma(t)\left(h - vt\right)\right]p_H}{\partial h}. \tag{29}$$

Consequently, we obtain for the phase saturation $S(z, t)$ the evolution equation

$$\frac{\partial S}{\partial t} = D\frac{\partial^2 S}{\partial z^2} - \left[v - \gamma(t)\left(h - vt\right)\right]\frac{\partial S}{\partial z}. \tag{30}$$

Its solution for the initial condition $S(z, t = 0) = \Theta(z)$ can be obtained by integration along the characteristics, or directly by the fact that p_H is a Gaussian characterized by mean vt and variance $\sigma_H^2(t)$ as

$$S = \frac{1}{2}\mathrm{erfc}\left(\frac{z - vt}{\sqrt{2\sigma_H^2}}\right). \tag{31}$$

C. Kadar-Parisi-Zhang Model

In order to obtain a saturation equation for the KPZ model, we close (14) by assuming that for moderate values of $\lambda \neq 0$ the conditional PDFs $p_{H_j|H_i}(h_j, t|h_i)$ and $p_{H_j,H_k|H_i}(h_j, h_k, t|h_i)$ are Gaussian as in the case of the EW model. Thus, the conditional mean is given by (21), where the C_{ij} are the height covariances of the KPZ model. The conditional height covariance is given by

$$\begin{aligned}\langle (H_j - \langle H_j|h_i\rangle)(H_k - \langle H_k|h_i\rangle)|h_i\rangle \\ = C_{jk} - \frac{C_{ij}C_{ik}}{C_{ii}}.\end{aligned} \tag{32}$$

Under this assumption, we obtain for the conditional drift (15)

$$V_i(h_i) = \frac{\mathcal{E}_i}{\sigma_H^2}\left(h_i - \langle H\rangle\right) + v + \mathcal{K}_i, \tag{33}$$

where $\mathcal{E}_i$ is defined by (23) and $\mathcal{K}_i$ is given by

$$\mathcal{K}_i = \frac{\lambda}{2}\frac{2C_{i+1i+1} - 2C_{i+1i-1}}{4\ell_0^2}. \tag{34}$$

This expression is obtained by using (32) for the conditional covariances in $\langle K_i(\mathbf{H})|h_i\rangle$ with $K_i(\mathbf{H})$ given by (7) and furthermore using that the statistics are stationary such that $C_{ii} = C_{jj}$ and $C_{ii+1} = C_{ii-1}$.

Now we turn to determining $\mathcal{E}_i$ and $\mathcal{K}_i$. To this end, we first consider the evolution equation for the the mean height $\langle H\rangle$. The averaging of (4) yields

$$\frac{\mathrm{d}\langle H\rangle}{\mathrm{d}t} = v + \mathcal{K}_i \tag{35}$$

The nonlinear KPZ term $\mathcal{K}_i$ causes a net interface displacement even in the absence of an external drift [6]; this is because transverse interface growth requires the addition of mass to the interface. The long time value of this drift is given by [24]

$$\mathcal{K}_i = \frac{\lambda D}{2\kappa}. \tag{36}$$

We define the effective interface velocity by

$$v_e = v + \frac{\lambda D}{2\kappa}. \tag{37}$$

In order to obtain a closed form expression for $\mathcal{E}_i$, we consider the evolution equation for the height fluctuation $H' = H - \langle H\rangle$, for which we obtain

$$\frac{\mathrm{d}H_i'}{\mathrm{d}t} = E_i(\mathbf{H}') + K_i(\mathbf{H}') - \mathcal{K}_i + \sqrt{2D}\xi_i(t). \tag{38}$$

Multiplication of the latter by H_i' and using the Ito rule gives

$$\frac{\mathrm{d}\sigma_H^2}{\mathrm{d}t} = \mathcal{E}_i + \langle H_i'[K_i(\mathbf{H}') - \mathcal{K}_i]\rangle + 2D. \tag{39}$$

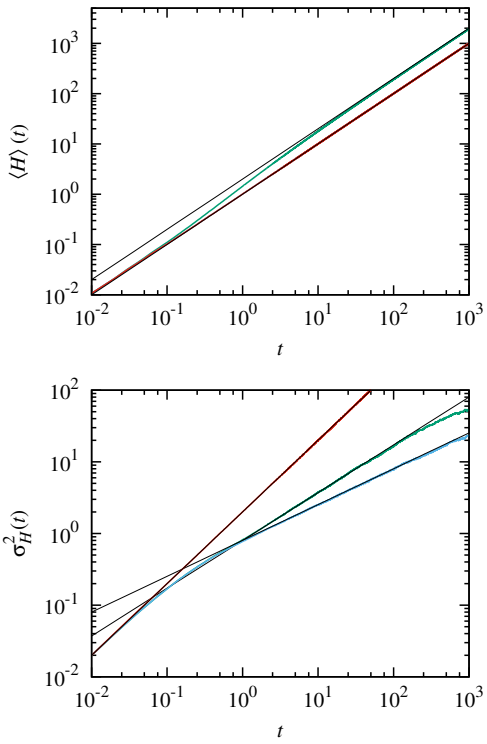

FIG. 1: Evolution of (top) the mean and (bottom) the variance of the interface height for (red) the random deposition model, (blue) the EW model and (green) the KPZ model. The results are obtained by numerical simulation of (4) for $\kappa = \lambda = 0$ and $v = 1$ (random deposition model), for $\kappa = 1$, $\lambda = 0$, and $v = 1$ (EW model), and $\kappa = 1$, $\lambda = 4$ and $v = 1$ (KPZ model), with $\ell_0 = 1$, $\Delta t = 10^{-2}$ and $a = 10^3$ in 10^2 realizations. Note that the red and blue line overlay each other in the top panel. The thin black lines in the top panel represent the mean interface heights $\langle H\rangle = vt$ for the random deposition and EW models and $\langle H\rangle = v_e t$ with v_e given by (37). The thin black lines in the bottom panel denote the diffusive behavior $\sigma_H^2 = 2Dt$, the behavior (28) for the EW model, and the behavior (41) for the KPZ model with $c_2 = 0.31$.

Under the assumption of Gaussianity, the second average on the right side is zero because it involves first and third order terms in the height fluctuations. Thus, we obtain as in the case of the EW model

$$\mathcal{E}_i = \frac{\mathrm{d}\sigma_H^2}{\mathrm{d}t} - 2D. \tag{40}$$

The height variance for the KPZ model is given by [24]

$$\sigma_H^2 = c_2\left(\frac{D\ell_0\lambda}{\kappa}t\right)^{2/3} \tag{41}$$

with c_2 a constant.

Thus, based on this Gaussian closure approximation, we obtain for the one-point point PDF $p_H(h, t)$ the closed

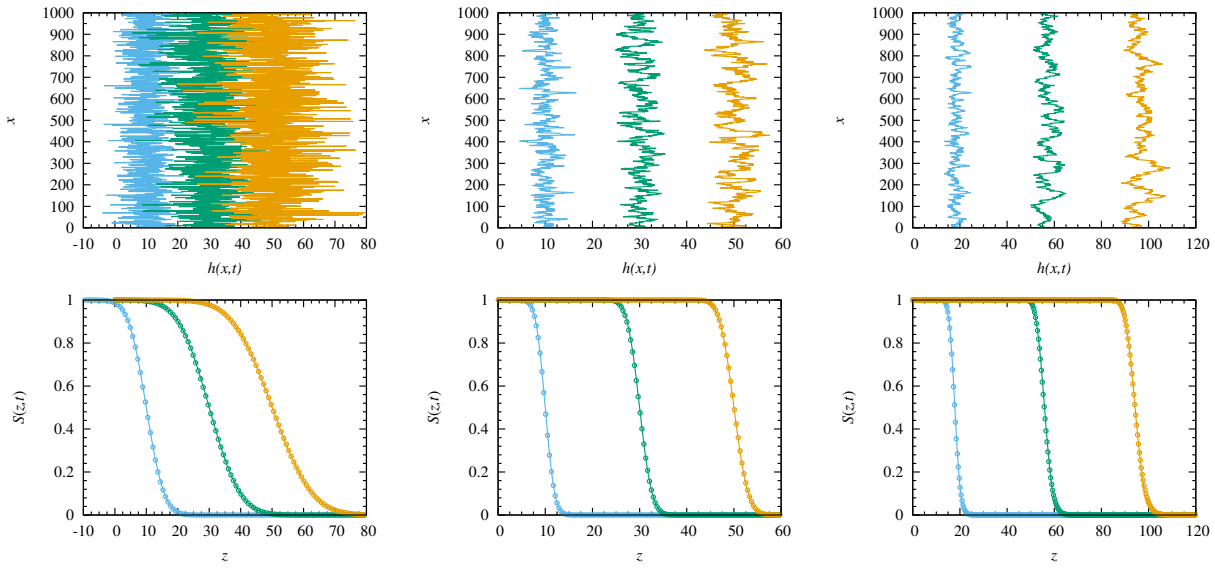

FIG. 2: Interfaces (top) and corresponding saturations (bottom) obtained with the (first column) random deposition model for $\kappa = \lambda = 0$ and $v = 1$ in (4), (middle column) the EW model for $\kappa = 1$, $\lambda = 0$, and $v = 1$ in (4), and (right column) the KPZ model with $\kappa = 1$, $\lambda = 4$ and $v = 1$ in (4) at times (from left to right) $t = 10$, 30 and 50. The circles in the bottom row indicate data from the numerical solution of (4) for $\ell_0 = 1$, $\Delta t = 10^{-2}$ and $a = 10^3$. These saturation profiles were obtained by spatial averaging along x and ensemble averaging over 10^2 realizations. The solid lines in the bottom row indicate the corresponding solutions (20), (31) and (44) for the saturation.

form evolution equation

$$\frac{\partial p_H}{\partial t} = D\frac{\partial^2 p_H}{\partial h^2} - \frac{\partial\left[v_e - \gamma(t)\,(h - v_e t)\right] p_H}{\partial h}, \qquad (42)$$

where $\gamma(t)$ is defined by (27) in terms of the height variance (41) of the KPZ model. The equation for the phase saturation is then obtained from (42) according to (3) as

$$\frac{\partial S}{\partial t} = D\frac{\partial^2 S}{\partial z^2} - \left[v_e - \gamma(t)(z - v_e t)\right]\frac{\partial S}{\partial z}. \qquad (43)$$

As in the case of the random deposition and EW models, its solution for a flat initial interface is given by a complementary error function as

$$S = \frac{1}{2}\mathrm{erfc}\left(\frac{z - v_e t}{\sqrt{2\sigma_H^2}}\right), \qquad (44)$$

where v_e is given by (37) and σ_H^2 by (41).

IV. SATURATION DYNAMICS

The evolution equation (19) for the random deposition model describes the evolution of an interface, whose width increases purely diffusively and whose mean position increases linearly with time with the constant velocity v, as illustrated in Figure 1. The evolution of a typical interface and the corresponding saturation profiles are illustrated in the first column of Figure 2.

The evolution of the interface and the corresponding saturation are different for the EW and KPZ models. In fact, the evolution equations (30) and (43) resemble those for scalar transport in fluid flow, under the competition of molecular diffusion and compression resulting from fluid deformation [25, 26]. The evolutions of the interface mean position and height variance are illustrated in 1. The height variances increase diffusively at short times until the interfacial smoothing due to the EW and KPZ terms, (6) and (7), starts dominating. Then, at later times it increases sub-diffusively as a result of the interfacial compression quantified by $\gamma(t)$. At asymptotic times, it converges towards a constant long time variance whose scaling with the lateral domain size a is given by $\sigma_H \propto a^{1/2}$ for both the EW and KPZ models [6] (asymptote not shown in Figure 1). Figure 2 illustrates the interface evolutions in the EW and KPZ models and the corresponding saturation profiles at different times. The circles in the bottom row of Figure 2 denote the data obtained by numerical simulations of (4), while the solid lines correspond to the analytical expressions (31) and (44) for the saturation profiles. Due to the interface in the EW and KPZ models, the saturation profiles are compressed in comparison to the random deposition model. The interfacial compression rate $\gamma(t)$ defined by (27) relates the stochastic mesoscale interface fluctuations to the macroscopic interface dynamics. In

the EW model it is given in leading order by

$$\gamma = \frac{\sqrt{2\pi\kappa}}{\ell_0} t^{-1/2} \tag{45}$$

while the KPZ model is in leading order characterized by the relatively weaker compression rate

$$\gamma = \frac{2D^{1/3}\kappa^{2/3}}{c_2\left(\ell_0\lambda\right)^{2/3}} t^{-2/3}. \tag{46}$$

Finally, we consider the issue of mass conservation for a constant flux of the deposited substance or, equivalently, for a constant fluid flux v_e in the KPZ and EW models. For the latter, $v_e = v$. Under this condition, the total amount of mass in the system,

$$I(t) \equiv \int_0^t S(z,t')\mathrm{d}t', \tag{47}$$

equals $I(t) = v_e t$. Indeed, integrating (43) over z and setting $S(0,t) = 1$, we obtain

$$\frac{\mathrm{d}I}{\mathrm{d}t} = v_e + \gamma(v_e t - I). \tag{48}$$

Since $I(0) = 0$, the solution of (48) is $I(t) = v_e t$. Thus, the mass is globally conserved. However, the saturation model (43) is not locally mass conservative, which follows from its divergence form,

$$\frac{\partial S}{\partial t} + \frac{\partial\left[v_e - \gamma(z - v_e t)\right] S}{\partial z} = D\frac{\partial^2 S}{\partial z^2} - \gamma(t)S. \tag{49}$$

The sink term $\gamma(t)S$ represents the mass transfer along the interface. It removes mass from locations where the interface is more advanced than its average position. Concurrently, the same mass is transferred from the boundary at $z = 0$ into the domain, which guarantees global mass conservation. This behavior is similar to evolution equations for scalar fronts transported by fluid flows and subjected to molecular diffusion and fluid deformation [25], as discussed above.

V. CONCLUSIONS

Macroscopic saturation equations are often based on local mass conservation and momentum balance over a control volume [27] and are therefore locally mass conserving. This is generally not the case for macroscopic descriptors emerging from stochastic mesoscale interface models, such as (2), because the saturation defined by (3) is given in terms of the cumulative probability of interface heights. Although the equation for the single-point PDF of the interface height is locally mass conservative, the equation satisfied by the cumulative distribution probability is not.

Nevertheless, for a given phenomenological description of the interface kinematics, a globally mass conserving saturation equation provides a valuable surrogate model of the true macroscopic dynamics. On the other hand, a macroscopic interface model may be used to infer mesoscale interface dynamics via the compression rate $\gamma(t)$, which connects the macroscopic interface dynamics with the mesoscale fluctuations. The derived methodology can be readily generalized to interfaces driven by colored noise [28].

Irrespective of the nonlinearity of the stochastic interface models, the macroscopic saturation dynamics are governed by linear partial differential equations, which include the salient features of the interfacial dynamics such as interface compaction. Stochastic interface dynamics and its equivalent macroscopic representations derived in this paper, provide a tool to predict the interface dynamics that results from various fluctuation and growth mechanisms.

Acknowledgments

MD acknowledges the funding from the European Research Council through the project MHetScale (Grant agreement no. 617511). IN acknowledges funding from DFG (Ne824/6-2 under the research unit MUSIS FOR 1083). DMT was supported in part by Defense Advanced Research Projects Agency under the EQUiPS program, the Air Force Office of Scientific Research under grant FA9550-12-1-0185 and by the National Science Foundation under grant DMS-1522799.

[1] P. Meakin, *Fractals, Scaling and Growth Far from Equilibrium*, Cambridge Nonlinear Science Series (Cambridge Univ. Press, New York, 1998).
[2] J. Koplik and H. Levine, Phys. Rev. B **32**, 280 (1985).
[3] M. Matsushita, J. Wakita, H. Itoh, I. Ràfols, T. Matsuyama, H. Sakaguchi, and M. Mimura, Physica A **249**, 517 (1998).
[4] A. A. Chernov, J. Cryst. Growth **264**, 499 (2004).
[5] C. P. E. Zollikofer and J. D. Weissmann, J. Anat. **219**, 100 (2011).
[6] A.-L. Barabasi and H. E. Stanley, *Fractal concepts in surface growth* (Cambridge Univ. Press, 1995).
[7] J. Merikoski, J. Maunuksela, M. Myllys, J. Timonen, and M. J. Alava, Phys. Rev. Lett. **90**, 024501 (2003).

[8] E. G. Flekkøy and D. H. Rothman, Phys. Rev. Lett. **75**, 260 (1995).
[9] P. Meakin, Phys. Rep. **235**, 189 (1993).
[10] S. Atis, A. Kumar Dubey, D. Salin, L. Talon, P. Le Doussal, and K. J. Wiese, Phys. Rev. Lett. **114**, 234502 (2015).
[11] T. Halpin-Healy and K. A. Takeuchi, J. Stat. Phys. **160**, 794 (2015).
[12] G. Løvoll, Y. Méheust, R. Toussaint, J. Schmittbuhl, and K. Måløy, Phys. Rev. E **70** (2004).
[13] R. Toussaint, G. Løvoll, Y. Méheust, K. J. Måløy, and J. Schmittbuhl, Europhys. Lett. **71**, 583 (2005).
[14] R. Toussaint, K. J. Måløy, Y. Méheust, G. Løvoll, M. Jankov, G. Schäfer, and J. Schmittbuhl, Vadose Zone J. (2012).
[15] M. Kardar, G. Parisi, and Y.-C. Zhang, Phys. Rev. Lett. **56**, 889 (1986).
[16] S. F. Edwards and D. R. Wilkinson, Proc. R. Soc. Lond. A **381**, 17 (1982).
[17] V. G. Miranda and F. D. A. Aarão Reis, Phys. Rev. E **77**, 031134 (2008).
[18] C. Dasgupta, J. M. Kim, D. M., and S. Das Sarma, Phys. Rev. E **55**, 2235 (1997).
[19] C.-H. Lam and F. G. Shin, Phys. Rev. E **57**, 6506 (1998).
[20] T. J. Newman and A. J. Bray, J. Phys. A: Math. Gen. **29**, 7917 (1996).
[21] A. L.-S. Chua, C. A. Haselwandter, C. Baggio, and D. D. Vvedensky, Phys. Rev. E **72**, 051103 (2005).
[22] H. Risken, *The Fokker-Planck Equation* (Springer, New York, 1996).
[23] D. B. Abraham and B. J. Upton, Phys. Rev. B **39**, 736 (1989).
[24] J. Krug, P. Meakin, and T. Halpin-Healy, Phys. Rev. A **45**, 638 (1992).
[25] W. E. Ranz, AIChE Journal **25**, 41 (1979).
[26] E. Villermaux and J. Duplat, Phys. Rev. Lett. **97**, 144506 (2006).
[27] J. Bear, *Dynamics of fluids in porous media* (American Elsevier, New York, 1972).
[28] P. Wang, A. M. Tartakovsky, and D. M. Tartakovsky, Phys. Rev. Lett. **110**, 140602 (2013).